

Optical properties of CdS nanoparticles upon annealing

V. Sivasubramanian*, A.K. Arora, M. Premila, C.S. Sundar, V.S. Sastry

Materials Science Division, Indira Gandhi Centre for Atomic Research, Kalpakkam 603 102, India

Received 20 May 2005; received in revised form 12 September 2005; accepted 10 October 2005

Available online 15 November 2005

Abstract

The metastable cubic phase of CdS has been found to be stabilized in the form of nanoparticles. Zinc-blende to Wurtzite structural transformation of CdS nanoparticles, synthesized using chemical precipitation, was investigated using X-ray diffraction (XRD), Raman, photoluminescence (PL) and infrared (IR) absorption spectroscopy. The nanocrystalline powder was annealed in argon atmosphere in the temperature range 473–773 K for 2 h at each temperature. The hexagonal fraction increased monotonically during annealing and the shape of the particle becomes anisotropic. PL spectra exhibited a marginal decrease in peak position for annealing up to 573 K and then an increase. In Raman spectra, the intensity of 1-LO phonon decreases while that of 2-LO phonon increases indicating an increase in electron–phonon interaction with increase in particle size. In addition to the Frohlich surface optical phonon mode and TO phonon mode, a new mode at 195 cm^{-1} is found in IR spectra, which is attributed to a defect-activated zone-boundary phonon. The changes in the optical properties are attributed to those arising from particle growth and structural transformation.

© 2005 Elsevier B.V. All rights reserved.

PACS: 61.46.+w; 78.30.-j; 78.55.-m

Keywords: Nanoparticles; Electron–phonon interaction; Frohlich mode and photoluminescence

1. Introduction

The electronic and optical properties of II–VI compound semiconductor nanoparticles have been extensively investigated in view of a wide variety of applications. With decrease in the particle size, dramatic modification of their electronic and optical properties takes place due to the three-dimensional quantum confinement of electrons and holes when the size of the particle approaches the Bohr radius of exciton [1,2]. In addition to the change in the electronic and optical properties, the structural behaviour also exhibits changes with reduction in the size of the particle. It is well known that bulk CdS has stable wurtzite (hexagonal) structure from room temperature to melting point. However, metastable cubic phase has been found in thin films and nanocrystalline powders [3,4]. Although the coexistence of cubic and hexagonal phases has been reported for CdS [5], a quantitative analysis of the volume

fractions and growth characteristics upon annealing was not carried out. Furthermore, nanoparticles of CdS have been reported to melt at a substantially lower temperature [6]. Although among semiconductor nanoparticles CdS has been most extensively studied, there is considerable diversity in the results that are reported. For example, the structural phase transition in CdS nanocrystalline thin films prepared by chemical bath deposition has been investigated using Raman [7], photoluminescence (PL) [2] and optical absorption [8]. A decrease in the band gap [8] and also the energy of the green PL [2] has been found upon annealing within the cubic phase. Bon et al. [8] tentatively attribute it to structural disorder prior to the cubic–wurtzite transition. Several PL studies have been reported on CdS nanoparticles prepared by various methods. For example, surface capped CdS nanoparticles [9] and those dispersed on GeO_2 [10] glass exhibit emission from recombination from defects occurring at the energies lower than the bulk band-edge. Also, certain aspects of the metastable cubic to the wurtzite phase transition upon annealing have not been well understood. Yellow-green

*Corresponding author. Tel.: +914427480347; fax: +914427480081.
E-mail address: shiva@igcar.ernet.in (V. Sivasubramanian).

emission from CdS nanoparticles in zeolites [11] and red emission from surface capped CdS [12] colloid has been attributed to Cd atoms and sulphur vacancies, respectively. On the other hand, PL spectra often exhibit well-defined peaks associated with band-edge luminescence and recombination at defects [13,14]. A new Raman peak at 278 cm^{-1} has been reported in the as-synthesized CdS films and after annealing at 350 and $450\text{ }^{\circ}\text{C}$ and not in the films annealed at other temperatures [7]. The origin of the peak is also not understood well. In order to understand the behaviour of optical and vibrational properties across cubic–wurtzite transition, we have carried out PL, Raman and infrared (IR) absorption studies on nanocrystalline powder samples of CdS after annealing at different temperatures. The X-ray diffraction (XRD) data are analysed quantitatively to obtain the hexagonal fraction, the average particle size and also its shape. Intensities of the fundamental and first overtone of the LO phonons are used for qualitative understanding of electron–phonon interaction in small particles. The features found in the IR absorption spectra are discussed in terms of surface and zone boundary phonon modes. The PL spectra are analysed to obtain the energies of direct interband transitions.

2. Experimental details

CdS nanoparticles have been synthesized by different methods like chemical precipitation in aqueous, nonaqueous media, hydrothermal methods [1,3,5]. The CdS nanoparticles were prepared by chemical precipitation in methanol. 4.3 g of $\text{Cd}(\text{NO}_3)_2 \cdot 4\text{H}_2\text{O}$ was dissolved in 200 ml of methanol. To this solution, 4.1 g of $\text{Na}_2\text{S} \cdot 12\text{H}_2\text{O}$ flakes were added slowly. Immediately after the addition of Na_2S , an orange precipitate is formed. The water of hydration present in cadmium nitrate and sodium sulphide was enough for the precipitation of CdS nanoparticles. The precipitate was filtered and then washed several times with water and methanol. Since annealing in air is known to cause the oxidation of CdS, the as-synthesized nanoparticles were annealed in argon atmosphere at 473, 573, 673 and 773 K for 2 h. Structural behaviour with increase in annealing temperature was monitored by XRD. Raman and PL spectra were excited with 488 nm line of an Ar-ion laser in the back scattering geometry. The signal was analysed using double grating monochromator (SPEX 14018) and detected using photomultiplier tube (Hamamatsu R943-02) in the photon counting mode. The Raman spectra were fitted to Lorentzian line shapes and PL spectra to Gaussians, respectively. IR absorption measurements were carried out using Bomem (DA-8) spectrophotometer.

3. Results and discussion

Powder XRD patterns of as-synthesized and annealed samples are shown in Fig. 1a. The as-synthesized samples were predominantly cubic as evident from characteristic (111), (220) and (311) peaks. However, one can see weak

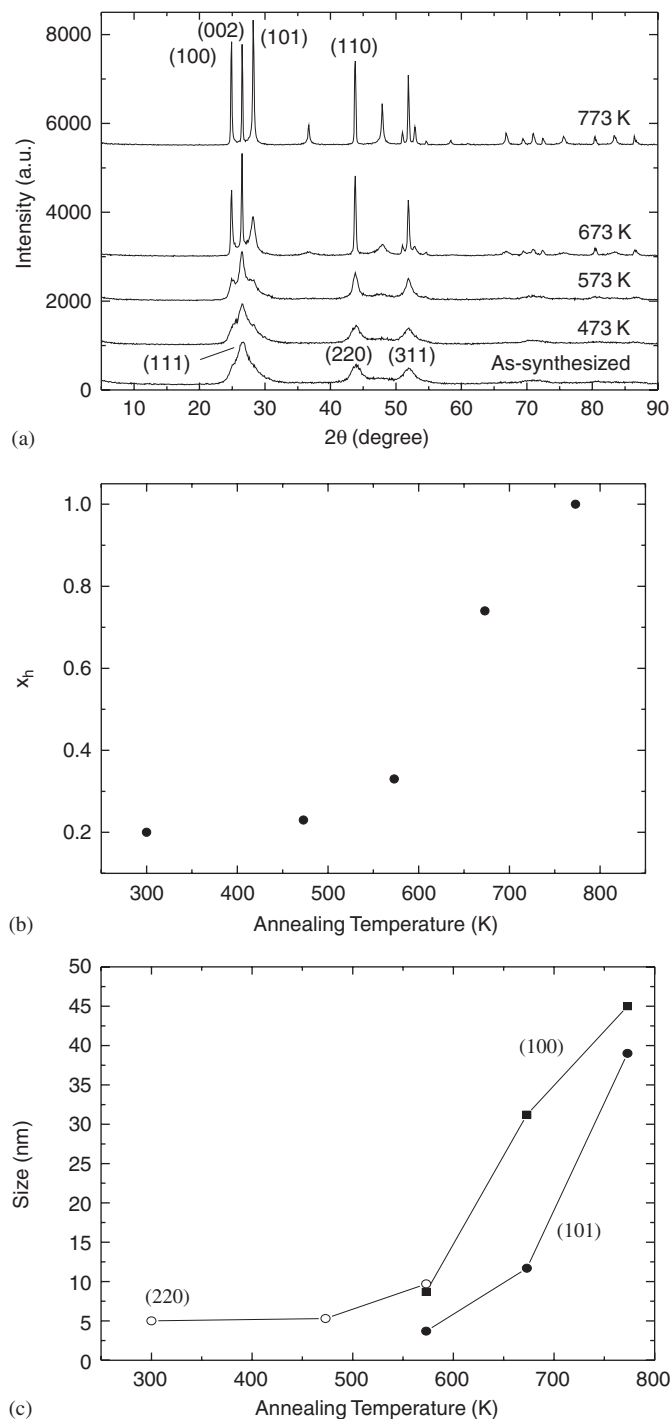


Fig. 1. (a) X-ray diffraction patterns of as-synthesized and annealed CdS nanoparticles. (b) Variation of hexagonal fraction (x_h) with annealing temperature. (c) Variation of size of the nanoparticles with annealing temperature. Open symbols: cubic, filled symbols: hexagonal.

shoulders corresponding to (100) and (101) peaks of wurtzite phase riding over the (111) peak of the cubic phase suggesting the presence of small fraction of wurtzite phase in as-synthesized sample. Furthermore, two peaks at $2\theta = 36.6$ and 47.8° , which are characteristic of the hexagonal phase, are not present in the case of as-synthesized sample. The intensities of these two peaks

show an increase with increase in annealing temperature. These results indicate that the relative content of hexagonal phase increases with increase in annealing temperature and for annealing at 773 K the structure becomes completely hexagonal. The fraction of hexagonal phase was estimated from the total integrated intensities of (100), (103) and (002), (110) lines. It may be pointed out that the (100) and (103) lines are unique to hexagonal; on the other hand, the 2θ positions of (002) and (110) lines of hexagonal phase have the same 2θ values as those for (111) and (220) lines of cubic phase, respectively. The integrated intensities were obtained by fitting the corresponding lines to Voigt function. The relative content of hexagonal phase (x_h) was calculated from the ratio $(I_{100} + I_{103})/(I_{002} + I_{110})$ assuming that the sample annealed at 773 K is fully hexagonal. The variation of hexagonal fraction (x_h) with annealing temperature is given in Fig. 1b. Note that the hexagonal fraction increases from 20% in the as-synthesized sample to 100% in the 773 K annealed sample. Also it can be noted that the evolution of diffraction peaks of the wurtzite phase is different for different peaks. For example, (100) and (110) peaks become rather sharp in the sample annealed at 573 K, whereas peaks (101) and (103) remain relatively broad. This suggests that growth of the wurtzite particles is anisotropic. Fig. 1c shows the sizes estimated from the Scherrer formula for the cubic and hexagonal phases using different reflections. One can see that the particle size in the wurtzite phase along (100) and (101) are very different. This suggests that growth in the $a - b$ plane is more than that along c -axis. This would result in an oblate spheroidal shape of the particle with the shorter dimension being along c -axis. The size of as-synthesized nanoparticles was 5 nm. With increase in annealing temperature, the size increased to 37 nm. It may be pointed out that the phase transition temperature (including melting) in the nanocrystalline systems have been found to be substantially lower than the corresponding bulk materials [15]. This is because the presence of significant fraction of atoms on the surface of the nanoparticle increases the total energy thereby making it less stable as compared to the bulk. Polycrystalline thin films of cubic-CdS have been reported to transform to hexagonal-CdS at about 720 K [16,17]. The present result suggests that the cubic-hexagonal transition temperature for CdS nanoparticle is understandable.

Raman spectra of CdS nanoparticles annealed at different temperature are shown in Fig. 2a. Two peaks are observed, 1-LO at 300 cm^{-1} and its overtone 2-LO at 600 cm^{-1} . Note that the Raman peaks do not shift significantly upon the transformation to the wurtzite phase. This is because the frequency of LO mode in cubic phase is nearly same as that of A_1 (LO) in the wurtzite phase [7]. On the other hand, the relative intensities of the 1-LO and 2-LO lines change as the size of the particle increase. As the size increases, 2-LO line becomes stronger while the 1-LO

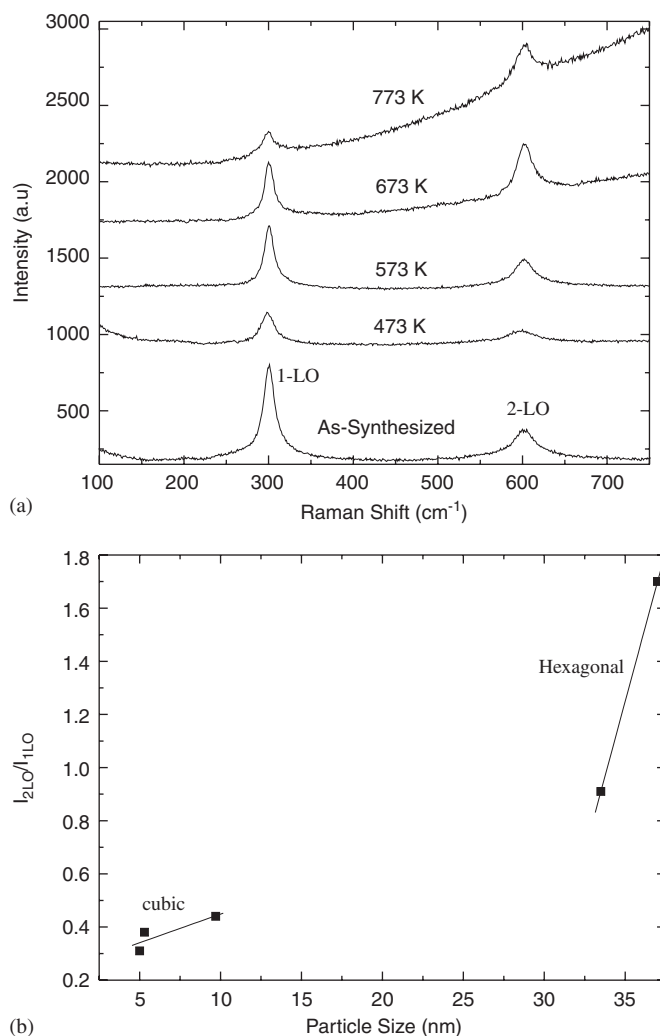


Fig. 2. (a) Raman spectra of CdS nanoparticles annealed at different temperatures. (b) Variation of I_{2LO}/I_{1LO} ratio with particle size. Cubic and hexagonal phases are indicated separately.

line becomes weaker in intensity. The variation of intensity ratio I_{2LO}/I_{1LO} as a function of particle size is shown in Fig. 2b. As discussed earlier, the particles have predominantly cubic structure for annealing up to 573 K, beyond which they become predominantly hexagonal. Hence the behaviour of Raman intensities of the fundamental and its overtone for two different structures are expected to be different. However, in either of the phases one finds that the ratio I_{2LO}/I_{1LO} decreases as the particle size reduces. I_{2LO}/I_{1LO} ratio is a measure of the strength of the electron-phonon interaction [18]. The present results thus suggest an increase in electron-phonon interaction as a function of particle size irrespective of the structure. Theoretical formalism of Schmidt-Rink et al. [19] has also indicated that the strength of electron-phonon interaction should decrease for small nanoparticles. A decrease in the electron-phonon coupling strength with decrease in particle size for InP quantum dots in the range 3.5–5.5 nm has also been reported [20]. This is in contrast to the resonance Raman scattering on $\text{CdS}_x\text{Se}_{1-x}$ nanoparticles [21] of sizes

between 2 and 3 nm and on ZnSe nanoparticles [22] of size <100 nm, that show the opposite behaviour. Stronger electron–phonon interaction is also predicted theoretically [23,24]. On the other hand, the Raman measurements on CdS nanoparticles of sizes between 1 and 7 nm [18] and CdSe nanoparticle of 4.5 nm size [25] suggest an increase of electron–phonon interaction as a function of particle size, similar to that found in the present study. The difference in the symmetry of LO phonons ($A_1 + E_1$) in the wurtzite phase with respect to that of the LO phonon (F_{2g}) in the cubic phase could be one of the reasons for substantially higher I_{2LO}/I_{1LO} ratio in the wurtzite phase. The change in the electron–phonon coupling (as seen from the LO intensity ratio) arises not only from the changes in the size but also due to the change in the structure. The electron–phonon coupling in bulk cubic-CdS is found to be much lower than that in hexagonal-CdS [26,27] because of the difference in the symmetries of LO phonons as well as that in the nature of the interband transitions in the two phases.

IR absorption spectra of the as-synthesized and annealed samples are shown in Fig. 3. The spectra were fitted with Lorentzian function. Two modes at 240 and 278 cm^{-1} along with very weak and broad peak around 195 cm^{-1} can be seen. The position and intensity of 240 and 275 cm^{-1} modes do not change with increase in particle size while the peak at 195 cm^{-1} show a small increase in intensity. The mode at 240 cm^{-1} is assigned to IR active transverse optical phonon mode [28]. There have been several studies of surface optical phonons using Raman and IR absorption spectroscopy [29–31]. Surface optical phonon modes in GaP microcrystals for the sizes in the range 50–430 nm have been observed in Raman scattering. The behaviour of the mode was explained by classical electro-magnetic theories [29]. Shoulders observed in the spectra of CdSe

have been attributed to the relaxation of $l = 0$ selection rule for non-spherical shape [30] and also to $l = 1$ Frohlich mode [32]. By neglecting mechanical boundary conditions and dispersion of bulk LO phonon modes, the shoulders observed in the Raman spectra at the position of the surface optical phonon modes were explained by the relaxation of $l = 0$ selection rule for the microcrystals with non-spherical shape. However, recent theory of Raman active confined optical modes developed for spherical quantum dots taking into account both mechanical and electrostatic and mechanical boundary conditions and considering the dispersion of LO phonon modes suggested that the observed shoulder in CdSe nanocrystals could be due to $l = 1$ Frohlich surface optical phonon mode [32]. On the other hand, Mlayah et al. [28] obtained good agreement for $l = 2$ surface optical phonon mode for the dependence of surface phonon modes on alloy composition x in $\text{CdS}_x\text{Se}_{1-x}$ nanoparticles. However, no surface optical phonon modes were observed for the CdSe nanocrystals ranging in size from 1.9 to 4.8 nm [33]. On the other hand, it has been shown that for sufficiently small sized nanocrystals, the vibrational modes of a quantum dot exhibit different characteristics depending on the boundary conditions involved [31]. For a nanoparticle embedded in a rigid matrix like glass, the theory predicts the appearance of multimode structure with several resonances allowed by the size. With increase in size of the nanoparticle, the multimode structure disappears and the spectrum has only one resonance at the Frohlich mode. For free standing nanoparticles, the theory predicts a size independent Frohlich mode when the dielectric constant satisfies the condition $\epsilon_s(\omega) = -(l+1)\epsilon_h/l$, where $l = 1, 2$, ϵ_h and ϵ_s are the optical dielectric constant of the host and the nanoparticle, respectively. The mode with $l = 1$ is called the Frohlich mode. It is a dipolar mode and corresponds to the uniform polarization of a microcrystal. Its frequency is given by $\omega_F = [(\epsilon_s\omega_{LO}^2 + 2\epsilon_h\omega_{TO}^2)/(\epsilon_s + 2\epsilon_h)]^{1/2}$. It has also been suggested that the vibrational modes of the nanoparticles can be observed through FIR absorption [31]. In the FIR absorption spectra as shown in Fig. 3, a prominent shoulder at 278 cm^{-1} was observed for all the samples. Using the parameters, $\omega_{LO} = 302 \text{ cm}^{-1}$, $\omega_{TO} = 238 \text{ cm}^{-1}$, $\epsilon_s = 5.32$ [28] and $\epsilon_h = 1$, the calculated value of ω_F turns out to be 285 cm^{-1} which is close that of the shoulder observed in FIR spectra. In the present study, the CdS nanoparticles are free standing and hence we assign the shoulder observed at 278 cm^{-1} in FIR spectra to the Frohlich mode. The position of broad peak near 195 cm^{-1} is found to be close to a zone boundary phonon at point K in the Brillouin zone [34]. Presence of defects in the nanocrystals can activate such a zone boundary phonon mode in IR spectrum. In view of this we assign this broad peak to defect-activated zone-boundary phonon.

The PL spectra of the CdS nanoparticles annealed at different temperatures are shown in Fig. 4. For the samples annealed up to 573 K, the spectra were fitted with single Gaussian, while for the annealing conditions at 673 and

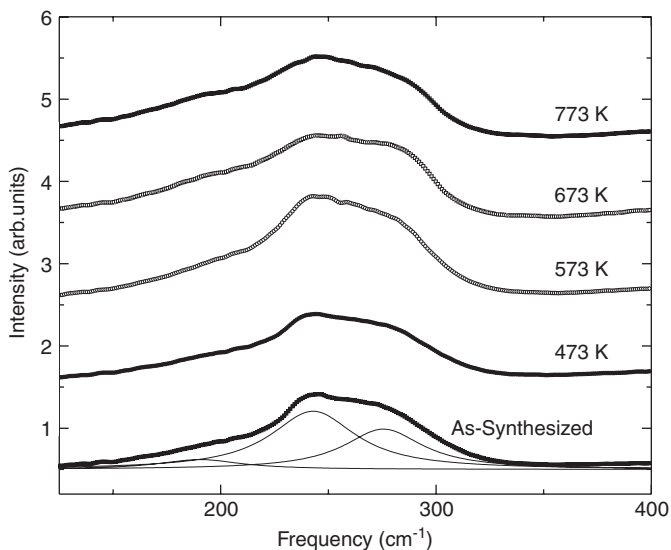


Fig. 3. IR absorption spectra of CdS nanoparticles annealed at different temperatures. The three components centered at 195, 240 and 278 cm^{-1} obtained by fitting are also shown for as-synthesized sample.

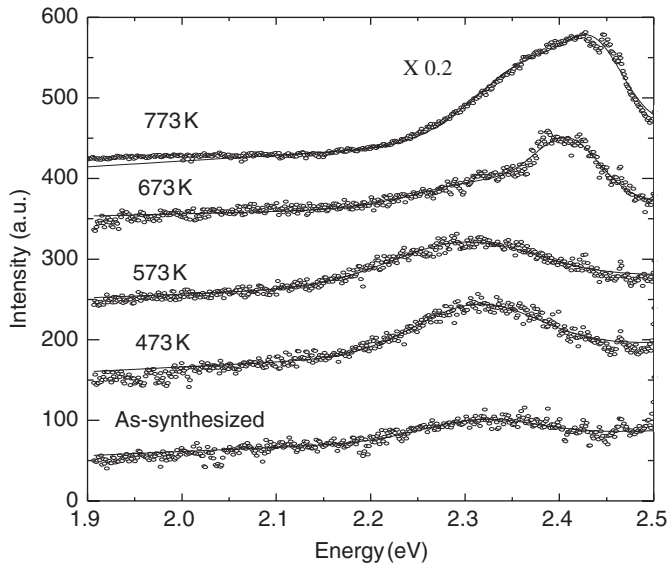


Fig. 4. Photoluminescence spectra of CdS nanoparticles annealed at different temperatures. Continuous lines are fitted curves.

773 K, with two Gaussians. PL peak energy as a function of annealing temperature is plotted in Fig. 5. The data of Angel et al. [2] are also shown for comparison. We find that in the cubic phase the position of PL peak remains nearly unchanged. On the other hand, Angel et al. found a large decrease in the energy of PL emission, which was not well understood and was tentatively attributed to the structural disorder prior to cubic–wurtzite transition [2]. We attribute this PL emission to arise from the radiative recombination from shallow donor to acceptor state. The marginal decrease of 17 meV in the peak position in the cubic phase may be due to the change in the confinement energy as a function of particle size. The PL emission from the shallow trap state also exhibit quantum confinement effect due to the strong mixing of its wave function with valence/conduction band [35]. One can also see from Fig. 5 that a new PL peak appears at 2.4 eV for annealing at 673 K and it increases to 2.44 eV for annealing at 773 K. This peak position could be due to the radiative recombination arising from shallow donor to valence band. One can also see that the shift in the PL peak position of the shallow acceptor state is nearly the same as that of the shift in the corresponding band edge PL in the wurtzite phase. The intensity of the shallow donor–acceptor peak is weaker in the wurtzite phase probably because of the change in the concentration of such defects. It may be pointed out that the large decrease in the PL energy as a function of annealing temperature reported earlier [2] was in cubic–CdS thin films having preferred orientation along (111) direction. On the other hand, the present results, which show only a marginal decrease in PL energy, are for self-standing nanocrystalline powder. In addition, we have found the particle growth to be anisotropic. Hence, the difference in the behaviour could be related to the preferred orientation and anisotropic shape of the particles.

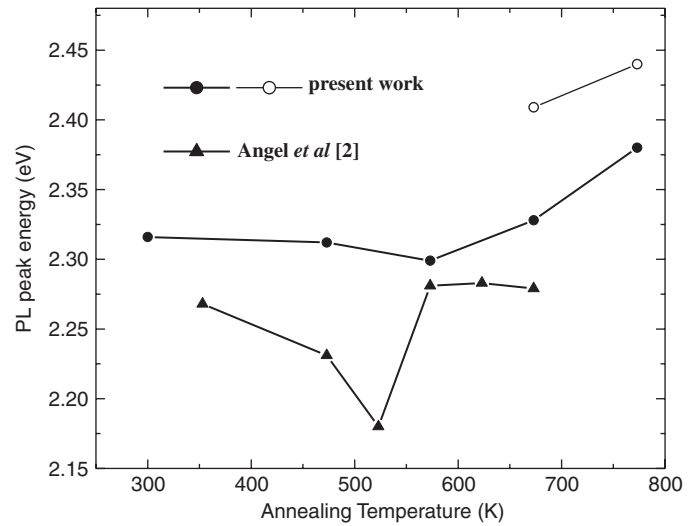


Fig. 5. Variation of PL peak energy with annealing temperature. The data of Angel et al. [2] is also shown for comparison.

4. Conclusions

We have investigated the structural phase transformation of as-prepared CdS nanoparticles upon annealing. With increase in particle size, the structure progressively changes from cubic to hexagonal. In the Raman spectra, the ratio of I_{2LO}/I_{1LO} increases monotonically during the annealing process, indicating an enhancement of electron–phonon coupling with increasing particle size for both cubic and hexagonal phases (although with different enhancement factors). This agrees with the majority of experimental results. PL peak position shows a marginal decrease for annealing up to 573 K. A defect-induced mode at 195 cm^{-1} , TO mode at 240 cm^{-1} and the Frohlich mode at 278 cm^{-1} are observed from IR absorption measurements.

Acknowledgements

Authors acknowledge Dr. M. Rajalakshmi for fruitful discussion, Dr. S.L. Mannan for interest in the work and Dr. Baldev Raj for support and encouragement.

References

- [1] R.J. Bandaranayake, G.W. Wen, J.Y. Lin, H.X. Jiang, C.M. Sorensen, *Appl. Phys. Lett.* 67 (1995) 831.
- [2] O.Z. Angel, A.E.E. Garcia, C. Falcony, R.L. Morales, R.R. Bon, *Solid State Commun.* 94 (1995) 81.
- [3] W. Wang, I. Germanenko, M.S. El-Shall, *Chem. Mater.* 14 (2002) 3028.
- [4] C.B. Murray, D.J. Norris, M.G. Bawendi, *J. Am. Chem. Soc.* 115 (1993) 8706.
- [5] Y. Li, F. Huang, Q. Zhang, Z. Gu, *J. Mater. Sci.* 35 (2000) 5933.
- [6] A.N. Goldstein, C.M. Echer, A.P. Alivisatos, *Science* 256 (1992) 1425.

- [7] O.Z. Angel, F. L.C. de Alvarado, J.A. Lopez, A.E. Esquivel, G.C. Puente, R.L. Morales, G.T. Delgado, *Solid State Commun.* 104 (1997) 161.
- [8] R.R. Bon, N.C.S. Inda, F.J.E. Beltran, M.S. Lerma, O.Z. Angel, C. Falcony, *J. Phys.: Condens. Matter* 9 (1997) 10051.
- [9] N. Herron, N. Wang, H. Eckert, *J. Am. Chem. Soc.* 112 (1990) 1322.
- [10] T. Arai, H. Fujumura, I. Umez, *Jpn. J. Appl. Phys.* 28 (1989) 484.
- [11] Y. Wang, N. Herron, *J. Chem. Phys.* 92 (1988) 4988.
- [12] H.S. Zhou, H. Sasahara, I. Honma, H. Komiyama, J.W. Haus, *Chem. Mater.* 6 (1994) 1534.
- [13] S. Okamoto, Y. Kanemitsu, H. Hosokawa, K. Murakoshi, S. Yanakida, *Solid State Commun.* 105 (1998) 7.
- [14] T.R. Ravindran, A.K. Arora, B. Balamurugan, B.R. Mehta, *NanoStruct. Mater.* 11 (1999) 603.
- [15] S.B. Qadri, E.F. Skelton, D. Hsu, A.D. Dinsmore, J. Yang, H.F. Gray, B.R. Ratna, *Phys. Rev. B* 60 (1999) 9191.
- [16] S. Soundeeswaran, O.S. Kumar, S.M. Babu, P. Ramasamy, R. Dhanasekaran, *Mater. Lett.* 59 (2005) 1795.
- [17] O.Z. Angel, J.J.A. Gill, R.L. Morales, H. Vargas, A.F. da Silva, *Appl. Phys. Lett.* 64 (1994) 291.
- [18] J.J. Shiang, S.H. Risbud, A.P. Alivisatos, *J. Chem. Phys.* 98 (1993) 8432.
- [19] Schmitt-Rink, D.A.B. Miller, D.S. Chemla, *Phys. Rev. B* 35 (1987) 8113.
- [20] M.J. Seong, O.I. Micic, A.J. Nozik, A. Mascarenhas, H.M. Cheong, *Appl. Phys. Lett.* 82 (2003) 185.
- [21] G. Scamarcio, V. Spagnolo, G. Venturi, M. Lugara, G.C. Righini, *Phys. Rev. B* 53 (1996) R10489.
- [22] S. Hayashi, H. Sanda, M. Agata, K. Yamamoto, *Phys. Rev. B* 40 (1989) 5544.
- [23] Al.L. Efros, A.I. Ekimov, F. Kozlowski, V. Petrova-Koch, H. Schmidbar, S. Shumilov, *Solid State Commun.* 78 (1991) 853.
- [24] S. Nomura, T. Kobayashi, *Phys. Rev. B* 45 (1992) 1305.
- [25] A.P. Alivisatos, T.D. Harris, P.T. Carrol, M.L. Steigerwald, L.E. Brus, *J. Chem. Phys.* 90 (1989) 3463.
- [26] O. Trujillo, R. Moss, K.D. Vuong, D.H. Lee, R. Noble, D. Finnigan, S. Orloff, E. Tenpas, C. Park, J. Fagan, X.W. Wang, *Thin Solid Films* 290–291 (1996) 13.
- [27] A. Gichuhi, B.E. Boone, C. Shannon, *J. Electroanal. Chem.* 522 (2002) 21.
- [28] A. Mlayah, A.M. Brugman, R. Carles, J.B. Renucci, M.Ya. Valakh, A.V. Pogolero, *Solid State Commun* 90 (1994) 567.
- [29] S. Hayashi, H. Kanamori, *Phys. Rev. B* 26 (1982) 7079.
- [30] M.C. Klein, F. Hache, D. Ricard, C. Flyzantis, *Phys. Rev. B* 42 (1990) 11123.
- [31] M.I. Vasilevskiy, *Phys. Rev. B* 66 (2002) 195326.
- [32] M.P. Chamberlain, C. Trallero-Giner, M. Cardona, *Phys. Rev. B* 51 (1995) 1680.
- [33] A. Tanaka, S. Onari, T. Arai, *Phys. Rev. B* 45 (1992) 6587.
- [34] H. Bilz, W. Kress, *Phonon Dispersion Relations in Insulators*, Springer, Berlin, 1979.
- [35] N. Chestnoy, T.D. Harris, R. Hull, L.E. Brus, *J. Phys. Chem.* 90 (1986) 3393.